Stability of the Toroidicity-induced Alfvén Eigenmode in JT-60U ICRF Experiments

G. Y. Fu, C. Z. Cheng

Princeton Plasma Physics Laboratory, Princeton University

P. O. Box 451

Princeton, New Jersey 08543, U.S.A.

H. Kimura, T. Ozeki and M. Saigusa

Naka Fusion Research Establishment, JAERI

Naka-machi, Naka-gun,Ibaraki-ken 311-01, Japan

(April 1, 1996)

Abstract

It is shown that the stability of toroidicity-induced Alfvén eigenmodes (TAE) in JT-60U ICRF experiments is strongly dependent on mode location. This dependence results in sequential excitation of high-n TAE modes as the central safety factor q drops in time.

52.35.Bj, 52.65.+z, 52.55.Pi

A key issue in tokamak reactor is the stability of toroidicity-induced Alfvén eigenmodes [1] (TAE) in the presence of fusion alpha particles [2]. The TAE instability can induce alpha particle loss, which could lead to damage to the tokamak wall. Previous experiments have shown that TAE modes can be strongly destabilized by fast ions in NBI-heated tokamak plasmas [3,4] and by fast minority trapped ions in ICRF-heated plasmas [5–8].

Recently, a series of experiments have been conducted to investigate the TAE modes excited by fast minority ions in JT-60U tokamak plasmas [6,7]. In these experiments, high-n TAE modes were observed during the ICRF heating phase, with mode number in the range of $5 > n > 13$. In particular, the TAE modes appears sequentially in mode number during a giant sawtooth. These interesting results might be relevant to ITER due to relatively large size and elongated shape of JT-60U tokamak plasmas

In this letter, we analyze the stability of TAE modes in ICRF-heated plasmas in JT-60U by using the global kinetic, magnetohydrodynamic (MHD) stability code NOVA-K [10,11], which has been used to assess the TAE stability in the recent TFTR DT experiments [12]. To destabilize TAE, the instability drive associated with the fast minority ions must overcome damping effects due to thermal particles. The NOVA-K code calculates perturbatively the fast particle drive, the Landau dampings of thermal electrons and ions and the collisional damping of trapped electron [11]. The nonperturbative radiative damping [13,14] is also calculated using a boundary layer method [15]. The continuum damping [16–18] is not included and its relevance will be discussed later. Here, we reiterate that the effects of finite orbit excursion from the flux surface due to magnetic drift are included in the calculation of fast ion drive [11]. This finite orbit width effect is particularly important in this study because the fast minority ions are trapped with large banana orbit width. All calculations are performed for realistic numerical equilibria based on experimental measurements.

The parameters and profiles used in this work are based on an ICRF discharge (E19332) in JT-60U [6,7] and are as follows: the major radius $R = 3.45m$, the minor radius $a = 1.0m$, the elongation $\kappa = 1.5$, the triagularity $\delta = 0.18$, the toroidal magnetic field $B_T = 3.8T$, the plasma current $I_p = 3.5MA$, the central electron density $n_e(0) = 2.8 \times 10^{13} cm^{-3}$, the

electron temperature $T_e(0) = 6.2keV$. The electron density profile, the thermal pressure profile and the safety factor q profile are

$$n_e = n_e(0)(1 - 0.88\Psi)^{0.5}, \tag{1}$$

$$P = P(0)(1 - \Psi)^2, \tag{2}$$

and

$$q = q_0 + \Psi \left[q_1 - q_0 + (q_1' - q_1 + q_0) \frac{(1 - \Psi_s)(\Psi - 1)}{\Psi - \Psi_s} \right] \tag{3}$$

where $\Psi_s = (q_1' - q_1 + q_0)/(q_0' + q_1' - 2q_1 + 2q_0)$, Ψ is the poloidal flux normalized to unity at plasma edge and zero at the magnetic axis, $q_0 = 0.8 \sim 1.0$, $q_1 = 3.78$, $q_0' = 0.60$ and $q_1' = 15.5$. The fast minority ion distribution function is assumed to be a Maxwellian in energy with a single pitch angle $\Lambda = \mu B/E = 1$. This is reasonable because the ICRF heating resonance surface is at the magnetic axis. The fast ion temperature profile is $T_h = T_h(0) \exp(-\Psi/\Psi_h)$ with $\Psi_h = 0.16$ and $T_h(0) = 1Mev$. The fast ion density profile is assumed to be constant. The volume-averaged fast ion beta is assumed to be $< \beta_h >= 5.0 \times 10^{-4}$, which is the estimated experimental threshold for TAE excitation.

Our numerical results indicate that the stability of TAE modes is strongly dependent on central safety factor $q(0)$. As $q(0)$ decreases, higher n TAE modes become unstable sequentially in mode number. These results are consistent with experimental observations [6,7].

Figure 1 shows the net growth rates as a function of $q(0)$ for $n = 5$, $n = 6$, and $n = 9$ modes. The growth rates of $n = 7$ and $n = 8$ modes, which are not plotted in Fig. 1, range between that of $n = 6$ and that of $n = 9$ mode. These results are obtained by subtracting the fast ion drive with the total damping rate of the mode. It is found that the radiative damping [15] is the dominating stabilizing mechanism. The electron Landau damping, the ion Landau damping and the collisional damping of trapped electrons are at least one order of magnitude smaller than the radiative damping, and are thus neglected. The results of

Fig. 1 show that the stability of TAE modes is a sensitive function of $q(0)$. As $q(0)$ decreases, the TAE modes become unstable one by one with increasing mode number. This is consistent with the experimental observations during the sawtooth stabilization phase in the ICRF-heated JT-60U discharges.

Physically, the strong dependence on $q(0)$ is due to the TAE mode structure. Figure 2 shows the amplitude of a $n = 9$ mode as a function of radial variable x for two $q(0)$ values where $x = \sqrt{\Psi}$. The modes are peaked near the continuum gap corresponding to $q = q_{gap} = (2n + 1)/2n$. We see that the mode peaks at larger radius for lower $q(0)$. The reason for the localization of the mode is weak magnetic shear near the center of the plasma. Since the distance between two neighboring continuum gaps is large when shear is small, the poloidal harmonics in the low shear region is weakly coupled to the modes at the next continuum gap location. In Fig. 3, we re-plot the net growth rates against the gap location x_{gap} where the mode is localized. The results indicate that the growth rates are sensitive to mode location and are maximized at $x_{gap} \sim 0.47$. We observe that the maximized value of x_{gap} is not sensitive to mode number, at least for the mode numbers considered here.

It should be noted that the effects of finite banana width (FBW) play a key role in determining the maximized value of x_{gap} for the instability drive. For JT-60U parameters, the banana width is about $\delta x \sim 0.2$, which is much larger than the typical TAE radial mode width (e.g., see Fig. 2). Figure 4 plots the fast particle drive for the $n = 9$ mode with and without FBW. We see that, without FBW, the drive is maximized at $x_{gap} = 0.32$. The FBW is stabilizing for $x_{gap} < 0.44$, while the opposite is true for $x_{gap} > 0.44$. This comes from two competing effects of FBW. On the one hand, the FBW is stabilizing for resonant particles which are near the mode peak. On the other hand, the FBW is destabilizing for resonant particles which are not close to the mode peak. The net effect of FBW depends on the mode location with respect to the location of maximum fast particle pressure gradient.

Finally, we discuss the stability thresholds of TAE modes. Figure 4 plots the critical fast

ion beta for instability versus $q(0)$. The critical $< \beta_h >$ varies from 1.0×10^{-4} for $n = 6$ mode to 2.0×10^{-4} for $n = 9$ mode. We see that these values are somewhat lower than the experimental estimate of $< \beta_h >= 5 \times 10^{-4}$ for the stability threshold. This indicates that the continuum damping, which is not included in this work, might play a role in determining the overall stability threshold, especially for lower n modes.

In conclusion, we have shown that the stability of TAE is strongly dependent on the mode location in JT-60U ICRF experiments. This result offers a plausible scenario for the sequential excitation of high-n TAE modes observed in the experiments.

Part of this work was done while one of the authors (G.Y. FU) was visiting the Japan Atomics Energy Research Institute at Naka, Japan. He thanks the hospitality of the host during his stay there. This work is supported by the U.S. Department of Energy under Contract No. DE-AC02-76-CHO-3073.

REFERENCES

[1] Cheng, C.Z., Chen, L., and Chance, M.S., Ann. Phys. (N. Y.) **161** (1985) 21.

[2] Fu, G.Y., and Van Dam, J.W., Phys. Fluids B**1** (1989) 1949.

[3] Wong K.L., et al., Phys. Rev. Lett. **66** (1991) 1874.

[4] Heidbrink, W.W., et al., Nucl. Fusion **31** (1991) 1635.

[5] Wilson, J.R., et al., in Proc. 14th Int. Conf. on Plasma Physics and Controlled Nuclear Fusion Research, Wurzburg, Germany, September, 1992 (International Atomic Energy Agency), IAEA-CN-56/E-2-2.

[6] Kimura, H., et al., Phys. Lett. A **199** (1995) 86.

[7] Saigusa, M., et al., Plasma Phys. Control. Fusion, **37** (1995) 295.

[8] Ali-Arshad, S. and Campbell, D.J., Plasma Phys. Control. Fusion **37** (1995) 715.

[9] Fredrickson, E., et al., in Proc. 15th Int. Conf. on Plasma Physics and Controlled Nuclear Fusion Research, Seville, Spain, October, 1994 (International Atomic Energy Agency), paper IAEA-CN/60/A-2-II-5.

[10] C. Z. Cheng, Phys. Reports **211** (1992) 1.

[11] Fu, G.Y., Cheng, C.Z., and Wong, K.L., Phys. Fluids B**5** (1993) 4040.

[12] Fu, G.Y., et al., Phys. Rev. Lett. **75** (1995) 2336.

[13] Mett, R., and Mahajan, S., Phys. Fluids B **4** (1992) 2885.

[14] Candy, J. and Rosenbluth, M.N., Phys. Plasmas **1** (1994) 356.

[15] Fu, G.Y., et al., submitted to Phys. Plasmas, 1995.

[16] Berk, H.L., Van Dam, J.W., Guo, Z., and Lindberg, D.M., Phys. Fluids B**4** (1992) 1806.

[17] Zonca, F. and Chen, L., Phys. Rev. Lett., **68**, (1992) 592.

[18] Rosenbluth, M.N., Berk, H.L., Lindberg, D.M., and Van Dam, J.W., Phys. Rev. Lett., **68** (1992) 596.

FIGURES

FIG. 1. The net growth rate of TAE modes as a function of $q(0)$ for mode number $n = 5$, $n = 6$ and $n = 9$.

FIG. 2. The amplitudes of poloidal harmonics versus plasma radius for the $n = 9$ TAE mode with two values of $q(0)$: (a)$q(0) = 0.95$ and (b)$q(0) = 0.90$.

FIG. 3. The net growth rate of TAE modes as a function of mode location x_{gap} formode number $n = 5$, $n = 6$ and $n = 9$.

FIG. 4. The fast ion drive versus the mode location for the $n = 9$ TAE mode with and without FBW effects.

FIG. 5. The critical volume-averaged fast ion beta versus $q(0)$ for $n = 6$ and $n = 9$ TAE modes.

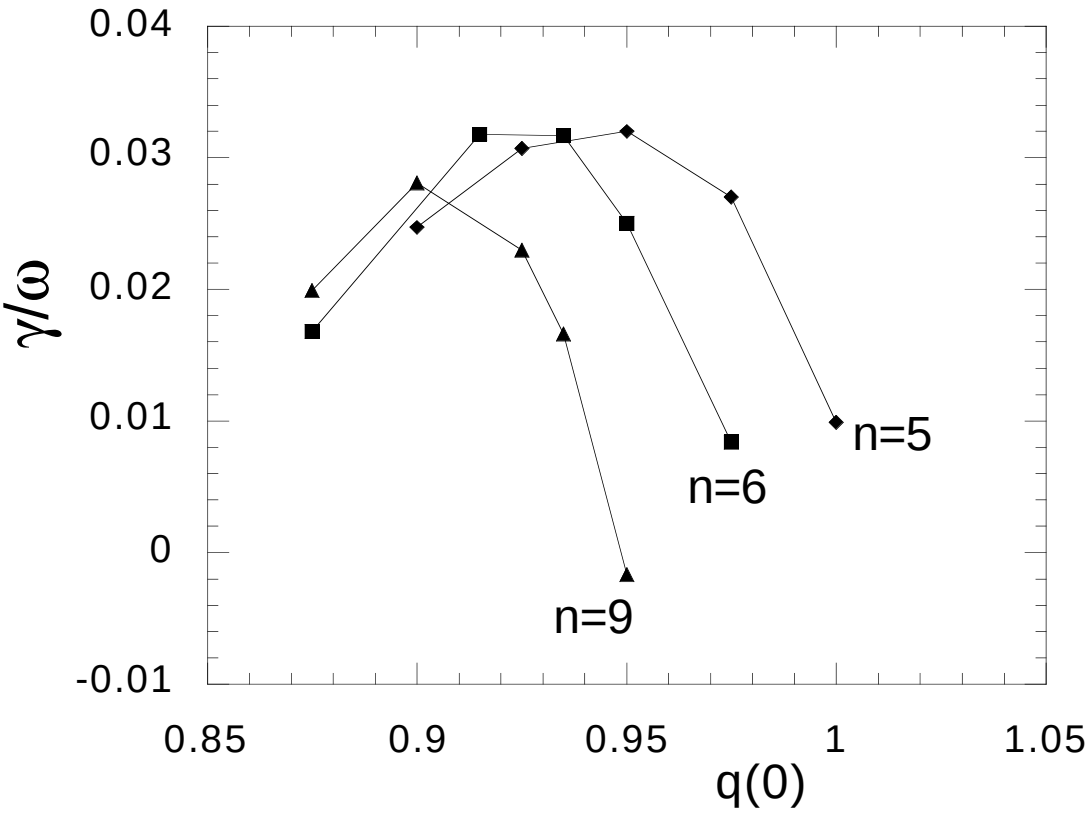

Fig. 1

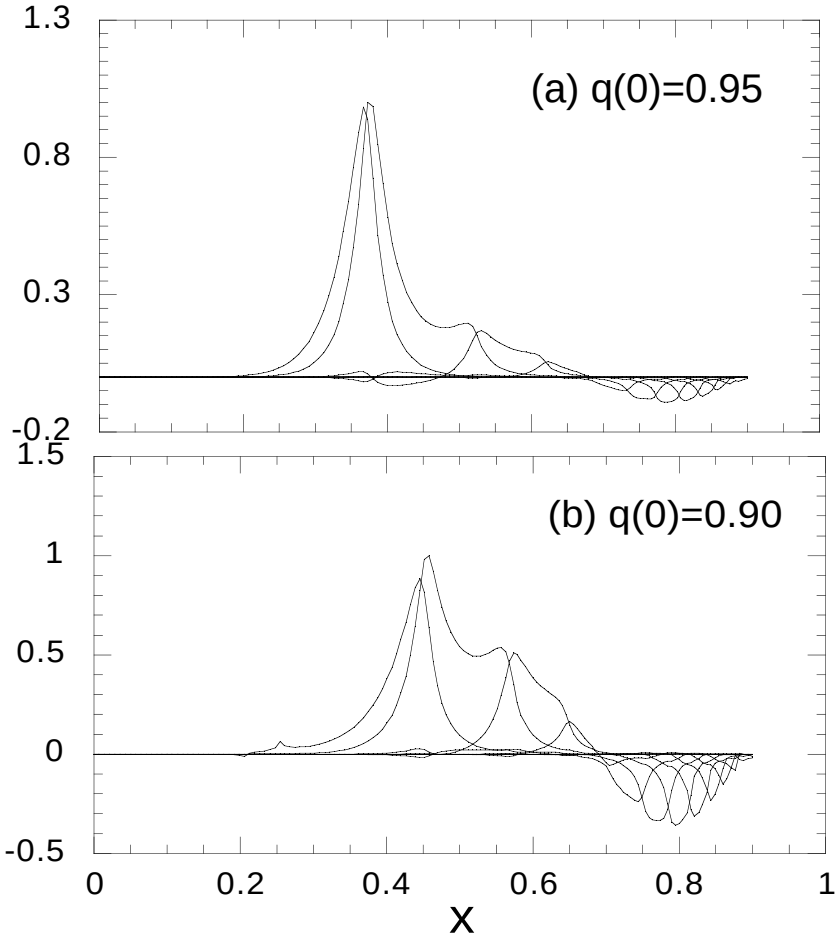

Fig. 2

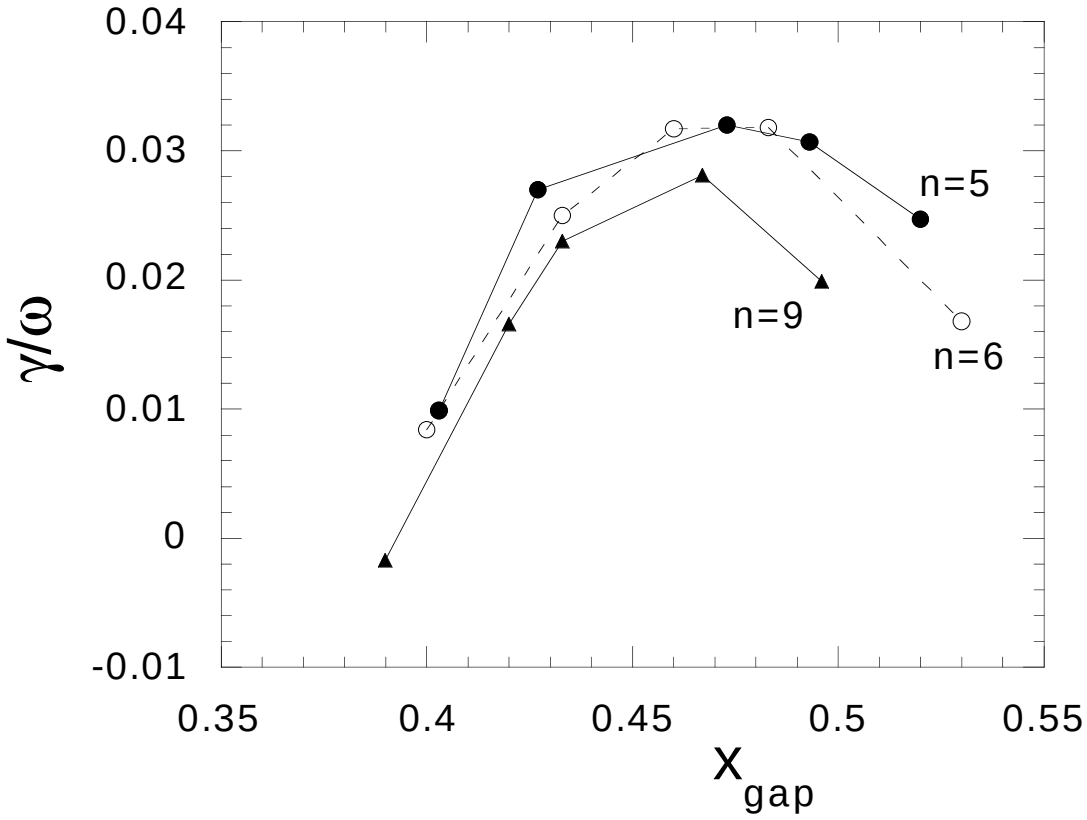

Fig. 3

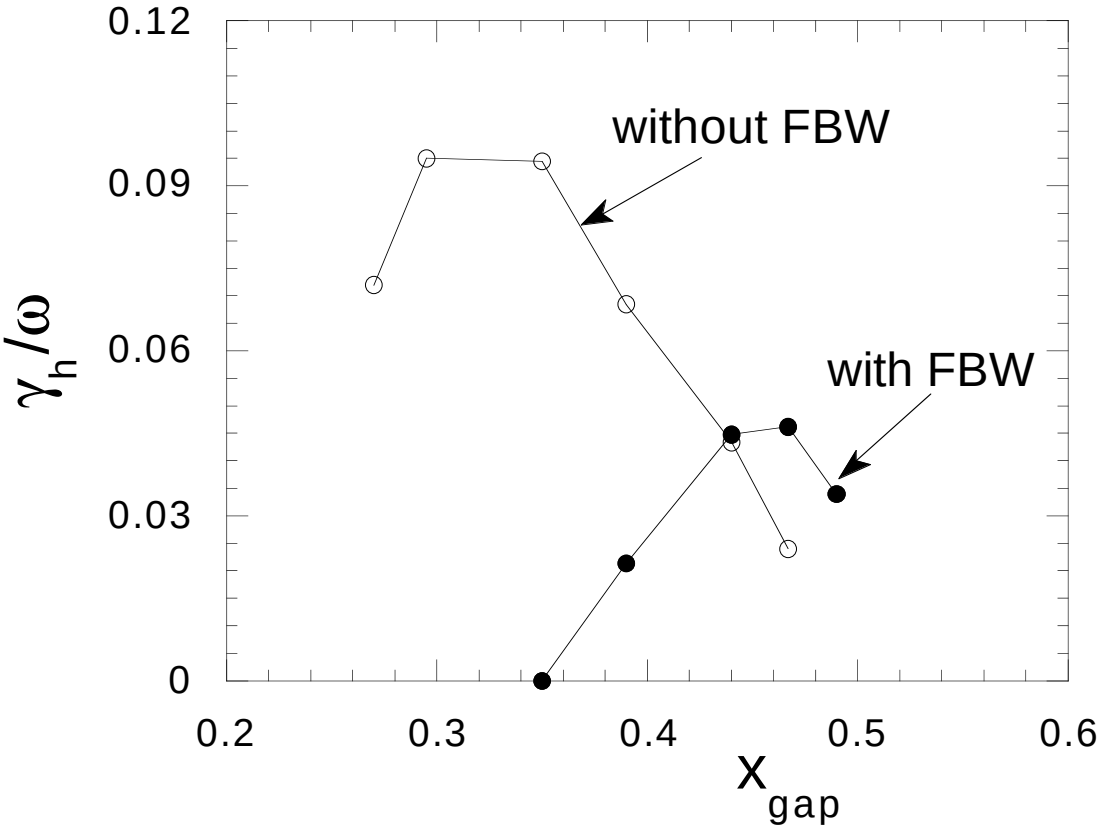
0.12
0.09
0.06
0.03
0
γ_h/ω
without FBW
with FBW
0.2
0.3
0.4
0.5
0.6
x_{gap}

Fig. 4

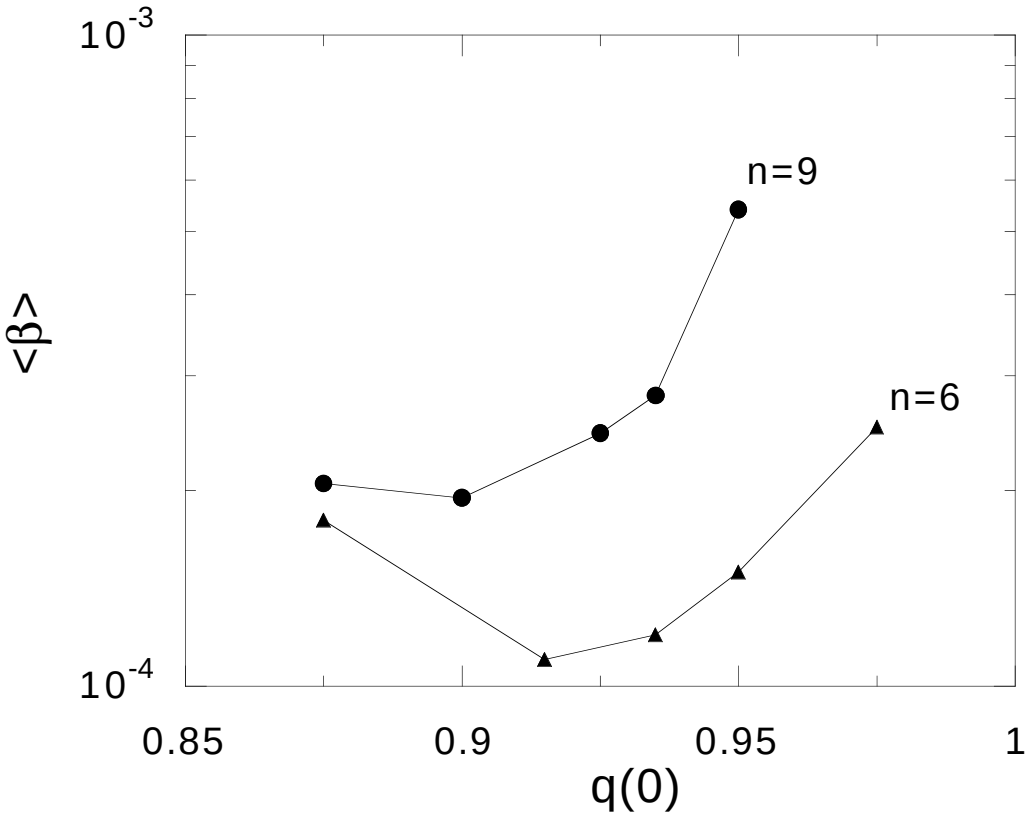

Fig. 5